Understanding the effects of climate warming on streamflow and active groundwater storage in an alpine catchment, upper Lhasa River

Lu Lin[a,b], Man Gao[c], Jintao Liu[a,b*], Jiarong Wang[a,b], Shuhong Wang[a,b*], Xi Chen[a,b,c], Hu Liu[d]

[a] *State Key Laboratory of Hydrology-Water Resources and Hydraulic Engineering, Hohai University, Nanjing 210098, People's Republic of China*

[b] *College of Hydrology and Water Resources, Hohai University, Nanjing 210098, People's Republic of China*

[c] *Institute of Surface-Earth System Science, Tianjin University, Tianjin 300072, People's Republic of China*

[d] *Linze Inland River Basin Research Station, Chinese Ecosystem Research Network, Lanzhou 730000, People's Republic of China*

* *Corresponding author. Tel.: +86-025-83787803; Fax: +86-025-83786606.*

E-mail address: jtliu@hhu.edu.cn (J.T. Liu).

Abstract

Climate warming is changing streamflow regimes and groundwater storage in cold alpine regions. In this study, a headwater catchment named Yangbajain in the Lhasa River Basin is adopted as the study area for assessing streamflow changes and active groundwater storage in response to climate warming. The results show that both annual streamflow and mean air temperature increase significantly at rates of about 12.30 mm/10a and 0.28 °C/10a during 1979-2013 in the study area. The results of gray relational analysis indicate that the air temperature acts as a primary factor for the increased streamflow. Due to climate warming, the total glacier volume has retreated by over 25% for the past half century, and the areal extent of permafrost has degraded by 15.3% in the recent twenty years. Parallel comparisons with other sub-basins in the Lhasa River Basin indirectly reveal that the increased streamflow at the Yangbajain station is mainly fed by the accelerated glacier retreat. Through baseflow recession analysis, we also find that the estimated groundwater storage that is comparable with the GRACE data increases significantly at the rates of about 19.32 mm/10a during these years. That is to say, as permafrost thawing, more spaces have been released to accommodate the increasing meltwater. The results in this study suggest that due to climate warming the impact of glacial retreat and permafrost degradation shows compound behaviors on storage-discharge mechanism, which fundamentally affects the water supply and the mechanisms of streamflow generation and change.

Keywords: Climate warming; Streamflow; Groundwater storage; Glacier retreat; Permafrost degradation; Tibetan Plateau

1. Introduction

Often referred to as the “Water Tower of Asia”, the Tibetan Plateau (TP) is the source area of major rivers in Asia, e.g., the Yellow, Yangtze, Lancang-Mekong, Yarlu Zangbo-Brahmaputra, and Nu-Salween, Indus Rivers (Cuo et al., 2014). The delayed release of water resources on the TP through glacier melt can augment river runoff during dry periods, giving it a pivotal role for water supply for downstream populations, agriculture and industries in these rivers (Viviroli et al., 2007; Pritchard, 2017). However, the TP is experiencing a significant warming period during the last half century (Kang et al., 2010; Liu and Chen, 2000). Along with the rising temperature, major warming-induced changes have occurred over the TP, such as glacier retreat (Yao et al., 2004; Yao et al., 2007) and frozen ground degradation (Wu and Zhang, 2008; Xu et al., 2019). Hence, it is of great importance to elucidate how climate warming influences hydrological processes and water resources on the TP.

In cold alpine catchments, glacier is known as “solid reservoir” that supplies water through streamflow, while frozen ground, especially permafrost, servers as an impermeable barrier to the interaction between surface water and groundwater (Immerzeel et al., 2010; Walvoord and Kurylyk, 2016; Rogger et al., 2017). Since the 1990s, most glaciers across the TP have retreated rapidly due to global warming and caused an increase of more than 5.5% in river runoff from the plateau (Yao et al., 2007). Meltwater is the key contributor to streamflow increase especially for headwater catchments with larger glacier coverage (>5%) (Bibi et al., 2018; Xu et al.,

2019). For example, the total discharge increase by 2.7%-22.4% mainly due to increased glacier melt that accounts for more than half of the total discharge increase in the upper Brahmaputra, i.e., Yarlu Zangbo (Su et al., 2016).

Meanwhile, in a warming climate, numerous studies suggested that frozen ground on the TP has experienced a noticeable degradation during the past decades (Cheng and Wu, 2007; Wu and Zhang, 2008; Zou et al., 2017). Frozen ground degradation can modify surface conditions and change thawed active layer storage capacity in the alpine catchments (Niu et al., 2011). Thawing of frozen ground increases surface water infiltration, supports deeper groundwater flow paths, and then enlarges groundwater storage, which is expected to have a profound effect on flow regimes (Kooi et al., 2009; Bense et al., 2012; Walvoord and Striegl, 2007; Woo et al., 2008; Ge et al., 2011; Walvoord and Kurylyk, 2016; Li et al., 2018; Wang et al., 2018). For example, Wang et al. (2018) suggested that ground ice may be a potential water source in continuous permafrost regions of central TP under global warming. However, in high mountainous regions in the TP, various terms of water recharge are quite complex especially in low elevations. In general, permafrost thawing in an arctic basin has resulted in a general upwards trend in groundwater contribution to streamflow of 0.7-0.9%/yr, however, with no pervasive change in total annual runoff (Walvoord and Striegl, 2007). Similar results have also been found in the central and northern TP (Liu et al., 2011; Niu et al., 2016; Xu et al., 2019). Moreover, a slowdown in baseflow recession was found in the northeastern and central TP (Niu et al., 2011;

Niu et al., 2016; Wang et al., 2017), in northeastern China (Duan et al., 2017), and in Arctic rivers (Lyon et al., 2009; Lyon and Destouni, 2010; Walvoord and Kurylyk, 2016).

Generally, in alpine regions, climate warming by triggering glacier retreat and permafrost thawing is changing hydrological processes of storage and discharge. However, direct measurement of the changing of permafrost depth or catchment aquifer storage is still difficult to perform at catchment scale (Xu et al., 2019; Staudinger, 2017; Käser and Hunkeler, 2016). Though its resolution and accuracy is relatively low, GRACE data has always been adopted in assessing total groundwater storage changes (Green et al., 2011). Quantitatively characterizing storage properties and sensitivity to climate warming in cold alpine catchments is desired for local water as well as downstream water management (Staudinger, 2017).

Xu et al. (2019) used a simple ratio of the maximum and minimum runoff to indirectly indicate the change of storage capacity as well as the effects of permafrost on recession processes. An alternative method, namely, recession flow analysis, can theoretically be used to derive the active groundwater storage volume to reflect frozen ground degradation in a catchment (Brutsaert and Nieber, 1977; Brutsaert, 2008). For example, the groundwater storage changes can be inferred by recession flow analysis assuming linearized outflow from aquifers into streams (Lin and Yeh, 2017). Due to the complex structures and properties of catchment aquifers, the linear reservoir model may not sufficient to represent the actual storage dynamics (Wittenberg, 1999;

Chapman, 1999; Liu et al., 2016). Hence, Lyon et al. (2009) adopted the nonlinear reservoir to fit baseflow recession curves for the derivation of aquifer attributes, which can be developed for inferring aquifer storage. Buttle (2017) used Kirchner's (2009) approach for estimating the dynamic storage in different basins and found that the storage and release of dynamic storage may mediate baseflow response to temporal changes. Generally, the classical recession flow analysis that is based on widely easily available hydrologic data is still widely used to provide important information on storage–discharge relationship of the basin (Patnaik et al., 2018).

In this study, the Yangbajain Catchment in the Lhasa River Basin is adopted as the study area. The catchment is experiencing glacier retreat and frozen ground degradation in response to climate warming. The main objectives of this study are (1) to assess the changes between surface runoff and baseflow in a warming climate; (2) to quantify active groundwater storage volume by recession flow analysis; (3) to analyze the impacts of the changes in active groundwater storage on streamflow variation. The paper is structured as follows. The section of Materials and Methods includes the study area, data sources and methods. The Results and Discussion sections present the changes in streamflow and its components, climate factors, and glaciers, and we will discuss the changing regimes of streamflow volume and baseflow recession in response to the changes of active groundwater storage and glaciers. The main conclusions are summarized in the section of Conclusions.

2. Materials and Methods

2.1. Study area

The 2,645 km^2 Yangbajain Catchment in the western part of the Lhasa River Basin (Figure 1a) lies between the Nyainqêntanglha Range to the northwest and the Yarlu-Zangbo suture to the south. In the central of the catchment, a wide and flat valley (Figure 1b) with low-lying terrain and thicker aquifers is in a half-graben fault-depression basin caused by the Damxung-Yangbajain Fault (Wu and Zhao, 2006; Yang et al., 2017). As a half graben system, the north-south trending Damxung-Yangbajain Fault (Figure 1b) provides the access for groundwater flow as manifested by the widespread distribution of hot springs (Jiang et al., 2016). The surface of the valley is blanketed by Holocene-aged colluvium, filled with the great thickness of alluvial-pluvial sediments from the south such as gravel, sandy loam, and clay. The vegetation in the catchment is characterized by alpine meadow, alpine steppe, marsh, shrub, etc, and meadow and marsh are mainly distributed in the valley and river source (Zhang et al., 2010).

Located on the south-central TP, the Yangbajain Catchment is a glacier-fed headwater catchment with significant frozen ground coverage (Figures 1b & 1c). A majority of glaciers were found along the Nyainqêntanglha Ranges (Figure 1b). Glaciers cover over ten percent of the whole catchment, making it the most glacierized sub-basin in the Lhasa River Basin. According to the First Chinese Glacier Inventory (Mi et al., 2002), the total glacier area was about 316.31 km^2 in 1960. The ablation period of the glaciers ranges from June to September with the glacier termini

at about 5,200 m (Liu et al., 2011). According to the new map of permafrost distribution on the TP (Zou et al., 2017), the valley is underlain by seasonally frozen ground (Figure 1c). It is estimated that seasonally frozen ground and permafrost accounts for about 64% and 36% of the total catchment area, respectively (Zou et al., 2017). The lower limit of alpine permafrost is around 4,800 m, and the thickness of permafrost varies from 5 m to 100 m (Zhou et al., 2000).

The catchment is characterized by a semi-arid temperate monsoon climate. The areal average annual air temperature of the Yangbajain Catchment is approximately -2.3°C with monthly variation from -8.6°C in January to 3.1°C in July (Figure 2). The average annual precipitation at the Yangbajain Station is about 427 mm. The catchment has a summer (June-August) monsoon with 73% of the yearly precipitation, while the rest of the year is dry with only 1% of the yearly precipitation occurring in winter (December-February) (Figure 2).

The average annual streamflow at the Yangbajain Station is 277.7 mm, and the intra-annual distribution of streamflow is uneven (Figure 2). In summer, streamflow is recharged mainly by monsoon rainfall and meltwater, and the volume of summer runoff accounts for approximately 63% of the yearly streamflow (Figure 2). The streamflow in winter with only 4% of the yearly streamflow (Figure 2) is only recharged by groundwater, which is greatly affected by the freeze-thawing cycle of frozen ground and the active layer (Liu et al., 2011).

2.2. Data

Daily streamflow and precipitation data at four hydrological Stations (Figure 1a) during the period 1979-2013 are collected from the Tibet Autonomous Region Hydrology and Water Resources Survey Bureau. The monthly meteorological data at three weather stations (Figure 1a) are obtained from the China Meteorological Data Sharing Service System (http://data.cma.cn/) for the years from 1979 to 2013. In this study, the method of meteorological data extrapolation by Prasch et al. (2013) is adopted to obtain the discretisized air temperature (with cell size as 1 km×1 km) of the Lhasa River Basin based on the air temperature of the three stations assuming a linear lapse rate. The mean monthly lapse rate is set to 0.44 °C/100m for elevations below 4,965 m and 0.78 °C/100m for elevations above 4,965 m in the catchment (Wang et al., 2015).

The glaciers and frozen ground data are provided by the Cold and Arid Regions Science Data Center (http://westdc.westgis.ac.cn/). The distribution, area and volume of glaciers are based on the First and Second Chinese Glacier Inventory in 1960 and 2009 (Mi et al., 2002; Liu et al., 2014) (Figure 1b). The distribution and classification of frozen ground (Figure 1c) are collected from the twice maps of frozen ground on the TP (Li and Cheng, 1996; Zou et al., 2017).

The latest Level-3 monthly mascon solutions (CSR, Save et al., 2016) was used to detect terrestrial water storage (TWS, total vertically-integrated water storage) changes for the period from January 2003 to December 2015 with spatial sampling of 0.5°×0.5° from the Gravity Recovery and Climate Experiment (GRACE) satellite.

The time series of 2003~2015 for snow water equivalent (SWE), total soil moisture (SM, layer 0~200cm) from the dataset (GLDAS_Noah2.1, https://disc.gsfc.nasa.gov/) were adopted for derivation of the groundwater storage (GWS) (Richey et al., 2015).

2.3. Methods

2.3.1. Statistical methods for assessing streamflow changes

The Mann-Kendall (MK) test, which is suitable for data with non-normally distributed or nonlinear trends, is applied to detect trends of hydro-meteorological time series (Mann, 1945; Kendall, 1975). To remove the serial correlation from the examined time series, a Trend-Free Pre-Whitening (TFPW) procedure is needed prior to applying the MK test (Yue et al., 2002). A more detailed description of the Trend-Free Pre-Whitening (TFPW) approach was provided by Yue et al. (2002).

Gray relational analysis was aimed to find the major climatic or hydrological factors that influenced an objective variable (Liu et al., 2005; Wang et al., 2013). In this paper, gray relational analysis is used to investigate the main climatic factors impacting the streamflow.

2.3.2. Baseflow separation

In this paper, the most widely used one-parameter digital filtering algorithm is adopted for baseflow separation (Lyne and Hollick, 1979). The filter equation is expressed as

$$q_t = \alpha q_{t-1} + \frac{1+\alpha}{2}\left(Q_t - Q_{t-1}\right) \quad (1)$$

$$b_t = Q_t - q_t \quad (2)$$

where q_t and q_{t-1} are the filtered quick flow at time step t and t-1, respectively; Q_t and Q_{t-1} are the total runoff at time step t and t-1; α is the filter parameter that ranging from 0.9 to 0.95; b_t is the filtered baseflow.

2.3.3. Determination of active groundwater storage

In this study, the active groundwater storage (also abbreviated as groundwater storage in the following context) is assumed as a storage that directly controls streamflow dynamics during rainless periods (Kirchner, 2009; Staudinger, 2017). Based on hydraulic groundwater theory, groundwater storage in a catchment can be approximated as a power function of baseflow rate at the catchment outlet (Brutsaert, 2008).

$$S = Ky^m \tag{8}$$

where y is the rate of baseflow in the stream, and S is the volume of active groundwater storage in the catchment aquifers (see in Figure 3). Here K, m are constants depending on the catchment physical characteristics, and K is the baseflow recession coefficient, which represents the time scale of the catchment streamflow recession process.

During dry season without precipitation and other input events, the conservation of mass equation can be represented as

$$\frac{dS}{dt} = -y \tag{9}$$

where t is the time. Substitution of equation (8) in equation (9) yields (Brutsaert and Nieber, 1977)

$$-\frac{dy}{dt} = ay^b \quad (10)$$

where dy/dt is the temporal change of the baseflow rate during recessions, and the constants a and b are called the recession intercept and recession slope of plots of $-dy/dt$ versus y in log-log space, respectively. In the storage discharge relationship, the aquifer responds as a linear reservoir if b=1, and as nonlinear reservoir if b≠1. In addition, with a fixed slope b, the changes in catchment aquifer properties by fitting the intercept a as a variable ban be observed (Rupp and Selker, 2006).

According to Gao et al. (2017), the parameters of K and m in equation (8) can be expressed by a and b, where $K = 1/\left[a\left(2-b\right)\right]$ and $m = 2-b$. Furthermore, the constants a and b can be determined through the technique of recession slope curves. In this study, the two constants are curve-fitted by using a nonlinear least squares regression through all data points of $-dy/dt$ versus y in log-log space for all years to avoid the difficulty of defining a lower envelop of the scattered points (Lyon et al., 2009). According to the values of a and b, K and m can be calculated. Thus the average groundwater storage S for dry season can be obtained through equation (8) based on average rate of baseflow.

3. Results

3.1. Assessment of streamflow changes

The annual streamflow of the Yangbajain Catchment shows an increasing trend at the 5% significance level with a mean rate of about 12.30 mm/10a over the period 1979-2013 (Table 1 and Figure 4a). Meanwhile, annual mean air temperature exhibits

248 an increasing trend at the 1% significance level with a mean rate of about 0.28 °C/10a
249 (Table 1 and Figure 5a). However, annual precipitation has a nonsignificant trend
250 during this period (Table 1 and Figure 5b).

251 As annual streamflow increases significantly, it is necessary to analyze to what
252 extent the changes in the two components (quick flow and baseflow) lead to
253 streamflow increases. Based on the baseflow separation method, the annual mean
254 baseflow contributes about 59% of the annual mean streamflow in the catchment. The
255 MK test shows that annual baseflow exhibits a significant increasing trend at the 1%
256 level with a mean rate of about 10.95 mm/10a over the period 1979-2013 (Table 1 and
257 Figure 4b). But the trend is statistically nonsignificant for annual quick flow in the
258 same period (Table 1). The increasing trends between the baseflow and streamflow
259 are very close, indicating that the increase in baseflow is the main contributor to
260 streamflow increases.

261 Furthermore, gray relational analysis is applied to the catchment to identify the
262 major climatic factors for the increasing streamflow. The result shows that the air
263 temperature has the higher gray relational grade at annual scale (Table 2). This
264 indicates that the air temperature acts as a primary factor for the increased streamflow
265 as well as the baseflow.

266 The annual streamflow and baseflow significantly increase due to the rising air
267 temperature over the period 1979-2013. However, there are diverse intra-annual
268 variation characteristics for streamflow as well as the two streamflow components

during the period. Streamflow in spring (March to May), autumn (September to November) and winter (December to February) show increasing trends at least at the 5% significance level (Figure 6a, 6c and 6d), while streamflow in summer (June to August) has a nonsignificant trend during this period (Figure 6b). Baseflow also increases significantly in spring, autumn and winter (Figure 6a, 6c and 6d). The trend is statistically nonsignificant for baseflow in summer (Figure 6b). Quick flow exhibits nonsignificant trend for all seasons (Table 1). As to the meteorological factors, mean air temperature in all seasons increase significantly at the 1% level especially during winter with the rate of about 0.51°C/10a (Table 1 and Figure 7), whereas precipitation in each season shows nonsignificant trend during these years (Table 1). The gray relational analysis shows that the air temperature is the critical climatic factor for the changes in streamflow and baseflow in all seasons (Table 2).

3.2. Estimation of groundwater storage by baseflow recession analysis

Daily streamflow and precipitation records in autumn and early winter (September to December) was adopted. In this dry season, hydrograph usually with little precipitation declines consecutively and smoothly. The fitted slope b is equal to 1.79 through the nonlinear least square fit of equation (10) for all data points of $-dy/dt$ versus y in log-log space during the period 1979-2013. Moreover, for each decade or year, the intercept a could be fitted by the fixed slope b=1.79. Then, the values of K and m for each decade or year can be determined. And the groundwater storage S for each year can be directly estimated from the average rate of baseflow during a

290 recession period through equation (8).

291 Figure 8 shows the results of the nonlinear least square fit for each decade's
292 recession data from the 1980s, 1990s and 2000s, respectively. As shown in Figure 8,
293 the recession data points and fitted recession curves of each decade gradually move
294 downward as time goes on. This indicates that, with a fixed slope *b*, the intercept *a*
295 gradually decreases and recession coefficient *K* increases accordingly. The values of
296 recession coefficient *K* for each decade are 77 $mm^{0.79}d^{0.21}$, 84 $mm^{0.79}d^{0.21}$ and 103
297 $mm^{0.79}d^{0.21}$. Furthermore, Figure 9a shows the inter-annual variation of recession
298 coefficient *K* during the period 1979-2013. In total, though there are some large
299 fluctuations or even a rather large decrease at the beginning of the 1990s, the overall
300 increasing trend of 7.70 $(mm^{0.79}d^{0.21})$/10a at a significance level of 5% is similar to the
301 results obtained from decade analysis. This long-term variation of recession
302 coefficient *K* from September to December indicates that baseflow recession during
303 autumn and early winter gradually slows down in the catchment.

304 According to the results of decade data fit (see in Figure 8), the mean values of
305 groundwater storage *S* estimated for each decade are 130 mm, 148 mm and 188 mm
306 for the 1980s, 1990s and 2000s. The inter-annual variation of groundwater storage *S*
307 is also similar with recession coefficient *K* (Figure 9a and 9b). The decreased trend of
308 anomalies changes of groundwater storage (*GWS*) estimated by the GRACE data is
309 consistent with the annual trend of *S* during 2003~2015 (Figure 9b). And the reduced
310 volume of groundwater between *GWS* and *S* are also comparable (~100-120 mm),

311 which has partly verified our estimations.

312 The trend analysis suggests that the groundwater storage *S* shows an increasing
313 trend at the 5% significance level with a rate of about 19.32 mm/10a during the period
314 1979-2013 (Figure 9b). The annual trend of groundwater storage *S* from 1979 to 2013
315 is consistent with the values across decades. This indicates that groundwater storage
316 has been enlarged. Through recent field investigations, we know that groundwater
317 level is rising. The increases of surface water and shallow groundwater storages are
318 changing the land cover. For example, the Normalized Difference Vegetation Index
319 (NDVI) is rising accordingly in the past twenty years (Figure 10). In fact, not only in
320 the study area but in the whole TP, surface water and groundwater storage are
321 increasing due to climate warming, and hence vegetation conditions have been
322 improved (Zhang et al., 2018; Khadka et al., 2018).

323 **4. Discussions**

324 The results have revealed that the increase of streamflow especially in dry season is
325 tightly related with climate warming. It is obviously that both glacier retreat and
326 frozen ground degradation in a warmer climate can significantly alter the mechanism
327 of streamflow. In the Yangbajain Catchment as well as the whole Lhasa River Basin,
328 it is experiencing a noticeable glacier retreat and frozen ground degradation during the
329 past decades (Table 3). For instance, according to the twice map of frozen ground
330 distribution on the TP (Li and Cheng, 1996; Zou et al., 2017), the areal extent of
331 permafrost in the Yangbajain catchment has decreased by 406 km^2 (15.3%) over the

past 22 years; the areal extent of seasonal frozen ground has increased by 406 km^2 (15.3%) with the corresponding degradation of permafrost.

According to the new map of permafrost distribution on the Tibetan Plateau (Zou et al., 2017), the coverages of permafrost and seasonally frozen ground in each sub-catchment (especially the Lhasa sub-catchments) are comparable to that in the Yangbajain Catchment; but the coverage of glaciers in the three catchments is far lower than that in the Yangbajain Catchment according to the First Chinese Glacier Inventory (Mi et al., 2002) (Table 3). The MK test showed that, in all the four catchments, the annual mean air temperature had significant increases at the 1% significance level (Figure 4) while the annual precipitation showed nonsignificant trends (Table 4). The annual streamflow of the three Lhasa, Pangdo and Tangga Catchments all had nonsignificant trends. The reason is that compared with the Yangbajain Catchment all the three larger sub-catchments as well as the whole Lhasa River Basin possess relatively smaller glacier coverage, in which summer rainfall contributes 48% of the total runoff according to Guan et al. (1984). While the annual streamflow of the Yangbajain Catchment showed an increasing trend at the 5% significance level with a mean rate of about 12.30 mm/10a during the period. Ye et al. (1999) stated that when glacier coverage is greater than 5%, glacier contribution to streamflow induced by climate warming starts to show up. As reported by Prasch et al. (2013), the contribution of accelerated glacial meltwater to streamflow would bring a significant increase in streamflow in the Yangbajain Catchment. Thus it is reasonable

353 to attribute annual streamflow increases to the accelerated glacier retreat as the
354 consequence of increasing annual air temperature in the Yangbajain Catchment.
355 Although permafrost degradation is not the controlling factor for the increase of
356 streamflow, a rational hypothesis is that increased groundwater storage *S* in autumn
357 and early winter is associated with frozen ground degradation, which can enlarge
358 groundwater storage capacity (Niu et al., 2016). Figure 3 depicts the changes of
359 surface flow and groundwater flow paths in a glacier fed catchment, which is
360 underlain by frozen ground under past climate and warmer climate, respectively. As
361 frozen ground extent continues to decline and active layer thickness continues to
362 increase in the valley, the enlargement of groundwater storage capacity can provide
363 enough storage space to accommodate the increasing meltwater that may percolate
364 into deeper aquifers (Figure 3). Then, the increase of groundwater storage in autumn
365 and early winter allows more groundwater discharge into streams as baseflow, and
366 lengthens the recession time as indicated by recession coefficient *K*. This leads to the
367 increased baseflow and slow baseflow recession in autumn and early winter, as is
368 shown in Figure 6c, 6d and Figure 9a. In the late winter and spring, the increase of
369 baseflow (Figure 6d and 6a) can be explained by the delayed release of increased
370 groundwater storage.
371 Thus, as the results of climate warming, river regime in this catchment has been
372 altered significantly. On the one hand, permafrost degradation is changing the aquifer
373 structure that controls the storage-discharge mechanism, e.g., catchment groundwater

storage increases at about 19.32 mm/10a. On the other hand, huge amount of water from glacier retreat is contributing to the increase of streamflow and groundwater storage. For example, the annual streamflow of the Yangbajain Catchment increases with a mean rate of about 12.30 mm/10a during the past 50 years. However, the total glacial area and volume have decreased by 38.05 km^2 (12.0%) and 1788 mm (26.2%) over the period 1960-2009 (Figure 11) according to the Chinese Glacier Inventories. Hence, the reduction rate of glacial volume is 9.46×10^7 m^3/a (about 357.7 mm/10a) on average during the past 50 years. In the ablation on continental type glaciers in China, evaporation (sublimation) always takes an important role, however, annul amount of evaporation is usually less than 30% of the total ablation of glaciers in the high mountains of China (Zhang et al., 1996). Given the 30% reduction in glacial melt, there is still a large water imbalance between melt-derived runoff and the actually increase of runoff and groundwater storage. Our results imply that more than 60% of glacial meltwater would be lost by subsurface leakage.

5. Conclusions

In this study, the changes of hydro-meteorological variables were evaluated to identify the main climatic factor for streamflow changes in the cryospheric Yangbajain Catchment. We find that the annual streamflow especially the annual baseflow increases significantly, and the rising air temperature acts as a primary factor for the increased runoff. Furthermore, through parallel comparisons of sub-basins in the Lhasa River Basin, we indirectly presumed that the increased streamflow in the

Yangbajain catchment is mainly fed by glacier retreat. Due to the climate warming, the total glacial area and volume have decreased by 38.05 km^2 (12.0%) and 4.73×10^9 m^3 (26.2%) in 1960-2009, and the areal extent of permafrost has degraded by 406 km^2 (15.3%) in the past 22 years. As a results of permafrost degradation, groundwater storage capacity has been enlarged, which triggers a continuous increase of groundwater storage at a rate of about 19.32 mm/10a. This can explain why baseflow volume increases and baseflow recession slows down in autumn and early winter.

At last we find that there is a large water imbalance (> 5.79×10^7 m^3/a) between melt-derived runoff and the actually increase of runoff and groundwater storage, which suggests more than 60% of the reduction in glacial melt should be lost by subsurface leakage. However, the pathway of these leakage is still an open question for further studies. More methods (e.g., hydrological isotopes) should be adopted to quantify the contribution of glaciers meltwater and permafrost degradation to streamflow, and to explore the change of groundwater storage capacity as frozen ground continues to degrade.

Acknowledgements:

This work was supported by the National Natural Science Foundation of China (NSFC) (grants 91647108, 91747203), the Science and Technology Program of Tibet Autonomous Region (2015XZ01432), the West Light Foundation of the Chinese Academy of Sciences (29Y929621) and the Special Fund of the State Key Laboratory of Hydrology-Water Resources and Hydraulic Engineering (no 20185044312).

References

Kooi, H., Ferguson, G., Bense, V. F.: Evolution of shallow groundwater flow systems in areas of degrading permafrost, Geophysical Research Letters, 36(22):297-304, 2009.

Bense, V. F., Kooi, H., Ferguson, G., and Read, T.: Permafrost degradation as a control on hydrogeological regime shifts in a warming climate, Journal of Geophysical Research Earth Surface, 117, F03036, doi:10.1029/2011JF002143, 2012.

Bibi, S., Wang, L., Li, X. P., Zhou, J., Chen, D. L., and Yao, T. D.: Climatic and associated cryospheric, biospheric, and hydrological changes on the Tibetan Plateau: A review, International Journal of Climatology, 38, e1-e17, doi:10.1002/joc.5411, 2018.

Brutsaert, W., and Lopez, J. P.: Basin-scale geohydrologic drought flow features of riparian aquifers in the southern Great Plains, Water Resources Research, 34(2), 233-240, 1998.

Brutsaert, W., and Nieber, J. L.: Regionalized drought flow hydrographs from a mature glaciated plateau, Water Resources Research, 13(3), 637-643, 1977.

Brutsaert, W.: Long-term groundwater storage trends estimated from streamflow records: Climatic perspective, Water Resources Research, 44(2), 114-125, doi:10.1029/2007WR006518, 2008.

Buttle, J. M.: Mediating stream baseflow response to climate change: the role of basin storage, Hydrological Processes, 32(1), doi:10.1002/hyp.11418, 2017.

Chapman, T.: A comparison of algorithms for stream flow recession and baseflow separation, Hydrological Processes, 13, 701-714, 1999.

Cheng, G. D., and Wu, T. H.: Responses of permafrost to climate change and their environmental significance, Qinghai-Tibet Plateau, Journal of Geophysical Research Earth Surface, 112, F02S03, doi:10.1029/2006JF000631, 2007.

443 Cuo, L., Zhang, Y. X., Zhu, F. X., and Liang, L. Q.: Characteristics and changes of
444 streamflow on the Tibetan Plateau: A review, Journal of Hydrology Regional
445 Studies, 2, 49-68, doi:10.1016/j.ejrh.2014.08.004, 2014.
446 Ding, Y. J., Zhang. S.Q., and Chen, R. S.: Introduction to hydrology in cold regions,
447 Science Press, Beijing, China, 2017 (In Chinese).
448 Duan, L., Man, X., Kurylyk, B.L., Cai, T.: Increasing winter baseflow in response to
449 permafrost thaw and precipitation regime shifts in northeastern China, Water, 9, 25,
450 doi:10.3390/w9010025, 2017.
451 Evans, S. G., and Ge, S.: Contrasting hydrogeologic responses to warming in
452 permafrost and seasonally frozen ground hillslopes, Geophysical Research Letters,
453 44, 1803-1813, doi:10.1002/2016GL072009, 2017.
454 Gao, M., Chen, X., Liu, J., Zhang, Z., and Cheng, Q.: Using two parallel linear
455 reservoirs to express multiple relations of power-law recession curves, Journal of
456 Hydrologic Engineering, 04017013, doi:10.1061/(ASCE)HE.1943-5584.0001518,
457 2017.
458 Ge, S., J. McKenzie, C. Voss, and Wu, Q.: Exchange of groundwater and
459 surface-water mediated by permafrost response to seasonal and long term air
460 temperature variation, Geophysical Research Letters, 38, L14402,
461 doi:10.1029/2011GL047911, 2011.
462 Guan, Z. H., Chen, C. Y., Kuang, Y. X., Fan Y. Q., Zhang, Y. S., and Chen, Z. M. et al.:
463 Rivers and Lakes in Tibetan. Rivers and lakes in Tibet. Beijing: Science and
464 Technology Press, 1984 (in Chinese).
465 Green, T. R., Taniguchi, M., Kooi, H., Gurdak, J. J., Allen, D. M., and Hiscock, K. M.,
466 et al.: Beneath the surface of global change: impacts of climate change on
467 groundwater, Journal of Hydrology, 405(3), 532-560,
468 doi:10.1016/j.jhydrol.2011.05.002, 2011.
469 Immerzeel, W. W., van Beek, L. P. H., and Bierkens, M. F. P.: Climate change will

affect the Asian water towers, Science, 328, 1382-1385, 2010.

Jiang, W., Han, Z., Zhang, J., and Jiao, Q.: Stream profile analysis, tectonic geomorphology and neotectonic activity of the Damxung-Yangbajain Rift in the south Tibetan Plateau, Earth Surface Processes and Landforms, 41(10), 1312-1326, doi:10.1002/esp.3899, 2016.

Kang, S. C., Xu, Y. W., You, Q. L., Flügel, W. A., Pepin, N., and Yao, T. D.: Review of climate and cryospheric change in the Tibetan Plateau, Environmental Research Letters, 5(1), 015101, doi:10.1088/1748-9326/5/1/015101, 2010.

Käser, D., and D. Hunkeler.: Contribution of alluvial groundwater to the outflow of mountainous catchments, Water Resources Research, 52, 680-697, doi:10.1002/2014WR016730, 2016.

Kendall, M. G.: Rank Correlation Methods, 4th ed, Charles Griffin, London, pp. 196, 1975.

Khadka, N., Zhang, G., and Thakuri, S.: Glacial Lakes in the Nepal Himalaya: Inventory and Decadal Dynamics (1977–2017). Remote Sensing, 10, 1913, doi:10.3390/rs10121913, 2018.

Kirchner, J.W.: Catchments as simple dynamical systems: catchment characterization, rainfall-runoff modeling, and doing hydrology backward, Water Resources Research, 45, W02429, doi:10.1029/2008WR006912, 2009.

Li, S., and Cheng, G.: Map of Frozen Ground on Qinghai-Xizang Plateau, Gansu Culture Press, Lanzhou, 1996.

Li, Z. J., Li, Z. X., Song, L. L., Ma, J. Z., and Song Y.: Environment significance and hydrochemical characteristics of suprapermafrost water in the source region of the Yangtze River, Science of the Total Environment, 644, 1141-1151, 2018.

Lin, K. T., and Yeh, H. F.: Baseflow recession characterization and groundwater storage trends in northern Taiwan, Hydrology Research, 48(6), 1745-1756, 2017.

Liu, J. S., Xie, J., Gong, T. L., Wang, D., and Xie, Y. H.: Impacts of winter warming

497 and permafrost degradation on water variability, upper Lhasa River, Tibet,
498 Quaternary International, 244(2), 178-184, doi:10.1016/j.quaint.2010.12.018, 2011.
499 Liu, J. T., Han, X. L., Chen, X., Lin, H., and Wang, A. H.: How well can the
500 subsurface storage-discharge relation be interpreted and predicted using the
501 geometric factors in headwater areas? Hydrological Processes, 30(25), 4826-4840,
502 doi:10.1002/hyp.10958, 2016.
503 Liu, Q. Q, Singh, V. P., and Xiang, H.: Plot erosion model using gray relational
504 analysis method, Journal of Hydrologic Engineering, 10, 288-294, 2005.
505 Liu, S. Y., Guo, W., and Xu, J., et al.: The Second Glacier Inventory Dataset of China
506 (Version 1.0), Cold and Arid Regions Science Data Center at Lanzhou, 2014,
507 doi:10.3972/glacier.001.2013.db.
508 Liu, X. D., and Chen, B. D.: Climatic warming in the Tibetan Plateau during recent
509 decades, International Journal of Climatology, 20(14), 1729-1742, 2000.
510 Lyne, V., and Hollick, M.: Stochastic time-variable rainfall-runoff modeling, Aust.
511 Natl. Conf. Publ. pp.89-93, 1979.
512 Lyon, S. W., and Destouni, G.: Changes in catchment-scale recession flow properties
513 in response to permafrost thawing in the Yukon River basin, International Journal
514 of Climatology, 30(14), 2138-2145, doi:10.1002/joc.1993, 2010.
515 Lyon, S. W., Destouni, G., Giesler, R., Humborg, C., Mörth, M., and Seibert, J., et al.:
516 Estimation of permafrost thawing rates in a sub-arctic catchment using recession
517 flow analysis, Hydrology and Earth System Sciences, 13(5), 595-604, 2009.
518 Mann, H.: Non-parametric test against trend, Econometrica, 13, 245-259, 1945.
519 Mi, D. S., Xie, Z. C., and Luo, X. R.: Glacier Inventory of China (volume XI: Ganga
520 River drainage basin and volume XII: Indus River drainage basin). Xi'an
521 Cartographic Publishing House, Xi'an, pp. 292-317, 2002 (In Chinese).
522 Niu, L., Ye, B. S., Li, J., and Sheng, Y.: Effect of permafrost degradation on
523 hydrological processes in typical basins with various permafrost coverage in

western China, Science China Earth Sciences, 54(4), 615-624, doi:10.1007/s11430-010-4073-1, 2011.

Niu, L., Ye, B., Ding, Y., Li, J., Zhang, Y., Sheng, Y., and Yue, G.: Response of hydrological processes to permafrost degradation from 1980 to 2009 in the upper Yellow River basin, China, Hydrology Research, 47(5), 1014-1024, doi:10.2166/nh.2016.096, 2016.

Patnaik, S., Biswal1, B., Kumar, D. N., Sivakumar, B.: Regional variation of recession flow power-law exponent, Hydrological Processes, 32, 866–872, 2018.

Prasch, M., Mauser, W., and Weber, M.: Quantifying present and future glacier melt-water contribution to runoff in a central Himalayan river basin, Cryosphere, 7(3), 889-904, doi:10.5194/tc-7-889-2013, 2013.

Pritchard, H. D.: Asia's glaciers are a regionally important buffer against drought, Nature, 545(7653), 169, doi:10.1038/nature22062, 2017.

Richey, A. S., Thomas, B. F., Lo, M.-H., Reager, J. T., Famiglietti, J. S., Voss, K., Swenson, S., and Rodell, M.: Quantifying renewable groundwater stress with GRACE, Water Resources Research, 51, 5217–5238, doi:10.1002/ 2015WR017349, 2015.

Rogger, M., Chirico, G. B., Hausmann, H. Krainer, K. Brückl, E. Stadler, P. and Blöschl, G.: Impact of mountain permafrost on flow path and runoff response in a high alpine catchment, Water Resources Research, 53, 1288-1308, doi:10.1002/ 2016WR019341, 2017.

Rupp, D. E., and Selker, J. S.: Information, artifacts, and noise in dQ/dt-Q recession analysis, Advances in Water Resources, 29(2), 154-160, 2006.

Save, H., Bettadpur, S., and Tapley, B. D.: High-resolution CSR GRACE RL05 masons, Journal of Geophysical Research: Solid Earth, 121, 7547–7569, doi.org/10.1002/2016JB013007, 2016.

Staudinger, M., Stoelzle, M., Seeger, S., Seibert, J., Weiler, M., and Stahl, K.:

551 Catchment water storage variation with elevation, Hydrological Processes, 31(11),
552 doi:10.1002/hyp.11158, 2017.
553 Su, F., Zhang, L., Ou, T., Chen, D., Yao, T., Tong, K., and Qi, Y.: Hydrological
554 response to future climate changes for the major upstream river basins in the
555 Tibetan Plateau. Global and Planetary Change, 136, 82-95, doi:10.1016/j.gloplacha.
556 2015.10.012, 2016.
557 Viviroli, D., Du¨rr, H. H., Messerli, B., Meybeck, M., and Weingartner, R.: Mountains
558 of the world, water towers for humanity: Typology, mapping, and global
559 significance, Water Resources Research, 43, W07447, doi:10.1029/2006WR005653,
560 2007.
561 Walvoord, M. A., and Kurylyk, B. L.: Hydrologic impacts of thawing permafrost-A
562 review, Vadose Zone Journal, 15(6), doi:10.2136/vzj2016.01.0010, 2016.
563 Walvoord, M. A., and Striegl, R. G.: Increased groundwater to stream discharge from
564 permafrost thawing in the Yukon River basin: Potential impacts on lateral export of
565 carbon and nitrogen, Geophysical Research Letters, 34(12), 123-134,
566 doi:10.1029/2007GL030216, 2007.
567 Wang, G., Mao, T., Chang, J., Song, C., and Huang, K.: Processes of runoff
568 generation operating during the spring and autumn seasons in a permafrost
569 catchment on semi-arid plateaus, Journal of Hydrology, 550, 307-317, 2017.
570 Wang, S., Liu, S. X., Mo, X. G., Peng, B., Qiu, J. X., Li, M. X., Liu, C. M., Wang, Z.
571 G., and Bauer-Gottwein, P.: Evaluation of remotely sensed precipitation and its
572 performance for streamflow simulations in basins of the southeast Tibetan Plateau,
573 Journal of Hydrometeorology, 16(6), 342-354, doi:10.1175/JHM-D-14-0166.1,
574 2015.
575 Wang, W. F., Wu, T. H., Zhao, L., Li R., Zhu X. F., Wang, W. R., Yang, S. H., Qin, Y.
576 H., and Hao, J. M.: Exploring the ground ice recharge near permafrost table on the
577 central Qinghai-Tibet Plateau using chemical and isotopic data, Journal of

578 Hydrology, 560, 220-229, 2018.
579 Wang, Y. F., Shen, Y. J., Chen, Y. N., and Guo, Y.: Vegetation dynamics and their
580 response to hydroclimatic factors in the Tarim River Basin, China, Ecohydrology,
581 6(6), 927-936, 2013.
582 Wang, Y. H., Yang, H. B., Gao, B., Wang, T. H., Qin, Y., and Yang, D. W.: Frozen
583 ground degradation may reduce future runoff in the headwaters of an inland river
584 on the northeastern Tibetan Plateau, Journal of Hydrology, 564, 1153-1164, 2018.
585 Wittenberg, H.: Baseflow recession and recharge as nonlinear storage processes,
586 Hydrological Processes, 13, 715-726, 1999.
587 Woo, M. K., Kane, D. L., Carey, S. K., and Yang, D.: Progress in permafrost
588 hydrology in the new millennium, Permafrost & Periglacial Processes, 19(2),
589 237-254, doi:10.1002/ppp.613, 2008.
590 Wu, Q. B., and Zhang, T. J.: Recent permafrost warming on the Qinghai-Tibetan
591 Plateau, Journal of Geophysical Research Atmospheres, 113, D13108,
592 doi:10.1029/2007JD009539, 2008.
593 Wu, Z. H., and Zhao, X. T.: Quaternary geology and faulting in the
594 Damxung-Yangbajain Basin, southern Tibet, Journal of Geomechanics, 12(3),
595 305-316, 2006 (in Chinese).
596 Xu, M., Kang, S., Wang, X., Pepin, N., and Wu H.: Understanding changes in the
597 water budget driven by climate change in cryospheric-dominated watershed of the
598 northeast Tibetan Plateau, China, Hydrological Processes, 1-19, doi:10.1002/hyp.
599 13383, 2019.
600 Yang, G., Lei, D., Hu, Q., Cai, Y., and Wu, J.: Cumulative coulomb stress changes in
601 the basin-range region of Gulu-Damxung-Yangbajain and their effects on strong
602 earthquakes, Electronic Journal of Geotechnical Engineering, 22(5), 1523-1530,
603 2017.
604 Yao, T. D., Pu, J. C., Lu, A. X., Wang, Y. Q., and Yu, W. S.: Recent glacial retreat and

its impact on hydrological processes on the Tibetan Plateau, China, and surrounding regions, Arctic, Antarctic, and Alpine Research, 39(4), 642-650, 2007.

Yao, T. D., Wang, Y. Q., Liu, S. Y., Pu, J. C., Shen, Y. P., and Lu, A. X.: Recent glacial retreat in high Asia in China and its impact on water resource in northwest China, Science in China, 47(12), 1065-1075, doi:10.1360/03yd0256, 2004.

Ye, B. S., Han, T. D., Ding, Y. J.: Some Changing Characteristics of Glacier Streamflow in Northwest China, Journal of Glaciolgy and Geocryology, 21(1):54-58, 1999 (in Chinese).

Yue, S., Pilon, P., Phinney, B., and Cavadias, G.: The influence of autocorrelation on the ability to detect trend in hydrological series, Hydrological Processes, 16(9), 1807-1829, doi:10.1002/hyp.1095, 2002.

Zhang, Y., Yao, T. D., and Pu, J. C.: The characteristics of ablation on continental-type glaciers in China, Journal of Glaciology and Geocryology, 18(2), 147-154, 1996 (in Chinese).

Zhang, Y., Wang, C., and Bai, W., et al.: Alpine wetland in the Lhasa River Basin, China, Journal of Geographical Sciences, 20(3): 375-388, 2010 (in Chinese).

Zhang, Z. X., Chang, J., and Xu, C. Y., et al.: The response of lake area and vegetation cover variations to climate change over the Qinghai-Tibetan Plateau during the past 30 years, Science of the Total Environment, 635, 443-451, 2018.

Zhou, Y. W., Guo, D. X., Qiu, G. Q., Cheng, G. D., and Li, S. D.: Permafrost in China, Science Press, Beijing, pp. 63-70, 2000 (In Chinese).

Zou, D., Zhao, L., Sheng, Y., and Chen, J., et al.: A new map of permafrost distribution on the Tibetan Plateau, The Cryosphere, 11, 2527-2542, doi:10.5194/tc-11-2527-2017, 2017.

630

Table 1. Mann-Kendall trend test with trend-free pre-whitening of seasonal and annual mean air temperature (°C), precipitation (mm), streamflow (mm), baseflow (mm) and quick flow (mm) from 1979 to 2013.

	Air temperature		Precipitation		Streamflow		Baseflow		Quick flow	
	Z_C	β (°C/a)	Z_C	β (mm/a)	Z_C	β (mm/a)	Z_C	β (mm/a)	Z_C	β (mm/a)
Spring	2.73**	0.026	0.90	0.290	3.05**	0.206	2.99**	0.147	0.98	0.042
Summer	2.63**	0.013	1.30	2.139	0.92	0.549	1.27	0.429	0.50	0.128
Autumn	2.65**	0.024	-0.68	-0.395	2.46*	0.546	2.96**	0.476	0.80	0.074
Winter	3.49**	0.051	-0.46	-0.014	3.08**	0.204	2.13*	0.145	1.39	0.016
Annual	4.48**	0.028	1.28	2.541	2.07*	1.230	2.70**	1.095	0.77	0.327

Comment: the symbols of Z_C and β mean the standardized test statistic and the trend magnitude, respectively; positive values of Z_C and β indicate the upward trend, whereas negative values indicate the downward trend in the tested time series; the symbols of asterisks *and ** mean statistically significant at the levels of 5% and 1%, respectively.

Table 2. Gray relational grades between the streamflow/baseflow and climate factors (precipitation and air temperature) in the Yangbajain Catchment at both annual and seasonal scales. Bold text shows the higher gray relational grade in each season.

	G_{oi} with the streamflow		G_{oi} with the baseflow	
	Precipitation	Air temperature	Precipitation	Air temperature
Spring	0.690	**0.778**	0.713	**0.789**
Summer	0.689	**0.784**	0.680	**0.776**
Autumn	0.653	**0.667**	0.648	**0.680**
Winter	0.742	**0.886**	0.748	**0.895**
Annual	0.675	**0.727**	0.665	**0.729**

631 Comment: G_{oi} is the gray relational grade between the streamflow/baseflow and climate factors. The importance of each influence factor can be determined by the
632 order of the gray relational grade values. The influence factor with the largest G_{oi} is regarded as the main stress factor for the objective variable.

633 Table 3. The coverage of glaciers and frozen ground in four catchments of the Lhasa River Basin

Stations	Area (km^2)	Glaciers(1960)		Glaciers(2009)		Permafrost (1996)		Permafrost (2017)		Seasonally frozen ground (1996)		Seasonally frozen ground (2017)	
		Area (km^2)	Coverage (%)	Area (km^2)	Coverage (%)	Area (km^2)	Coverage (%)	Area (km^2)	Coverage (%)	Area (km^2)	Coverage (%)	Area (km^2)	Coverage (%)
Lhasa	26233	349.26	1.3	347.14	1.3	10535	40.2	9783	37.3	15698	59.8	16450	62.7
Pangdo	16425	345.24	2.1	339.90	2.1	8666	52.7	8242	50.2	7762	47.3	8184	49.8
Tangga	20152	348.12	1.7	342.27	1.7	10081	50.0	9432	46.8	10071	50.0	10720	53.2
Yangbajain	2645	316.31	12.0	278.26	10.5	1352	51.1	946	35.8	1293	48.9	1699	64.2

634

635 Table 4. Mann-Kendall trend test with trend-free pre-whitening of annual mean air temperature (°C), precipitation (mm) and streamflow (mm) in
636 four catchments of the Lhasa River Basin

	Air temperature		Precipitation		Streamflow	
	Z_C	β (°C/a)	Z_C	β (mm/a)	Z_C	β (mm/a)
Lhasa	6.07**	0.028	1.16	1.581	1.09	1.420
Pangdo	6.19**	0.026	0.89	1.435	0.30	0.223
Tangga	7.35**	0.021	1.48	2.005	-0.62	-0.531
Yangbajain	4.48**	0.028	1.28	2.541	2.07*	1.230

637

Figure captions

Figure 1. (a) The location, (b) elevation distribution, and (c) glacier and frozen ground distribution (Zou et al., 2017) in the Yangbajain Catchment of the Lhasa River Basin in the TP.

Figure 2. Seasonal variation of streamflow (*R*), mean air temperature (*T*), and precipitation (*P*) in the Yangbajain Catchment.

Figure 3. Diagram depicting surface flow and groundwater flow due to glacier melt and permafrost thawing under (a) past climate and (b) warmer climate.

Figure 4. Variations of annual (a) streamflow and (b) baseflow from 1979 to 2013.

Figure 5. Variations of annual (a) mean air temperature and (b) precipitation from 1979 to 2013.

Figure 6. Variations of seasonal streamflow and baseflow in (a) spring, (b) summer, (c) autumn, and (d) winter from 1979 to 2013.

Figure 7. Variations of seasonal mean air temperature in (a) spring, (b) summer, (c) autumn, and (d) winter from 1979 to 2013.

Figure 8. Recession data points of $-dy/dt$ versus y and fitted recession curves by decades in log-log space. The black point line, dotted line, and solid line represent recession curves in the 1980s, 1990s, and 2000s, respectively.

Figure 9. Variations of (a) the recession coefficient K and (b) groundwater storage S from 1979 to 2013.

Figure 10. Variations of annual NDVI from 1998 to 2013 in the catchment.

659 **Figure 11.** The total area and volume of glaciers in the Yangbajain Catchment in 1960

660 and 2009.

661

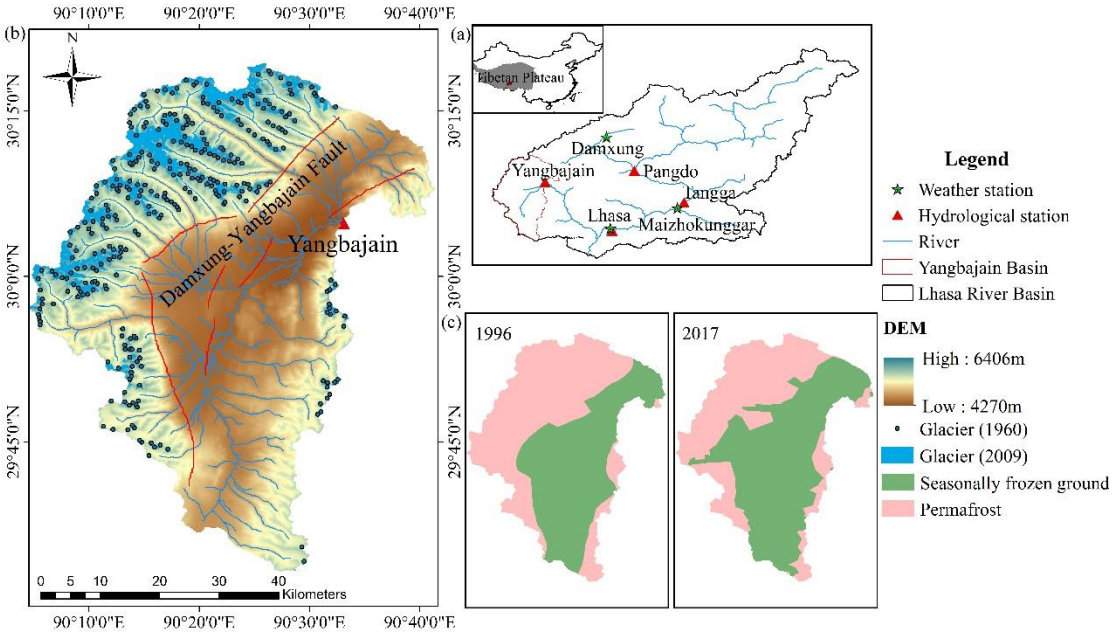

662

663 **Figure 1.** (a) The location, (b) elevation and glacier distribution for the twice Chinese

664 Glacier Inventory, only the location of glacier snouts in 1960 were provided in the

665 first Chinese Glacier Inventory, and the boundaries of glaciers were shown in the

666 second Chinese Glacier Inventory, and (c) twice maps of frozen ground distribution

667 (Li and Cheng, 1996; Zou et al., 2017) in the Yangbajain Catchment.

668

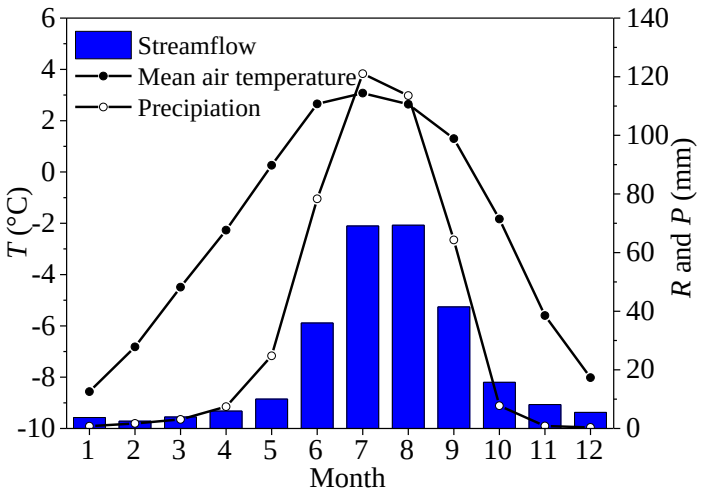

669

670 **Figure 2.** Seasonal variation of streamflow (*R*), mean air temperature (*T*), and

671 precipitation (*P*) in the Yangbajain Catchment.

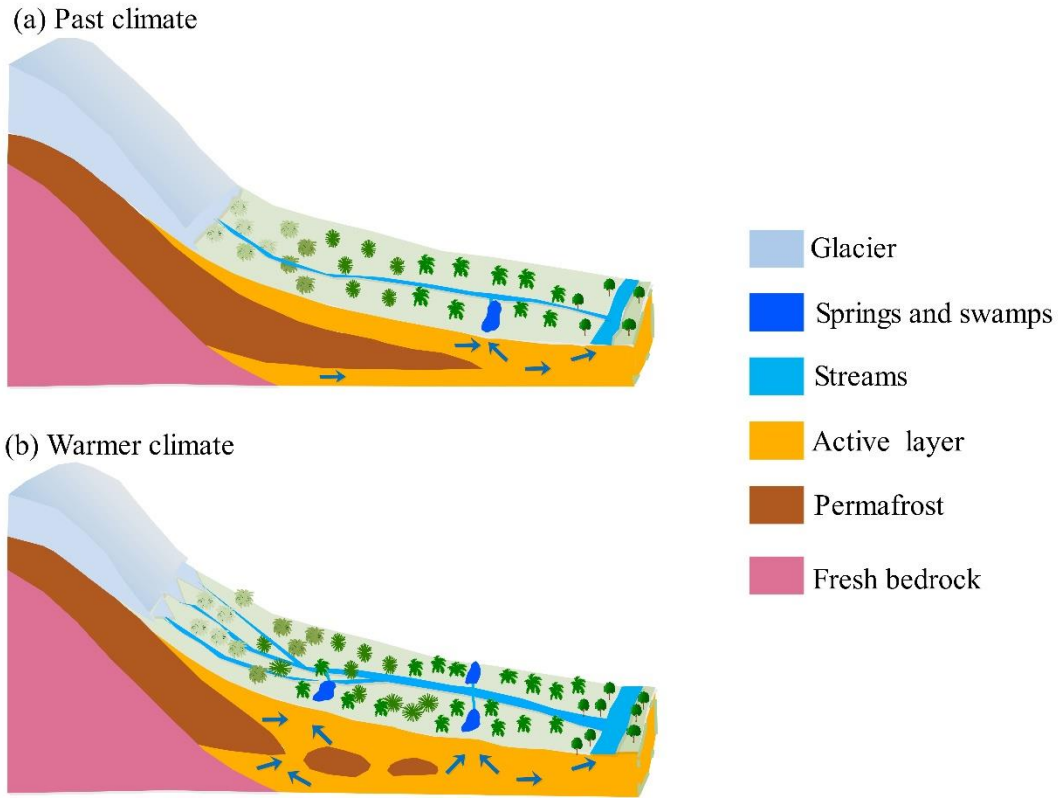

672

673 **Figure 3.** Diagram depicting surface flow and groundwater flow due to glacier melt

674 and permafrost thawing under (a) past climate and (b) warmer climate.

675

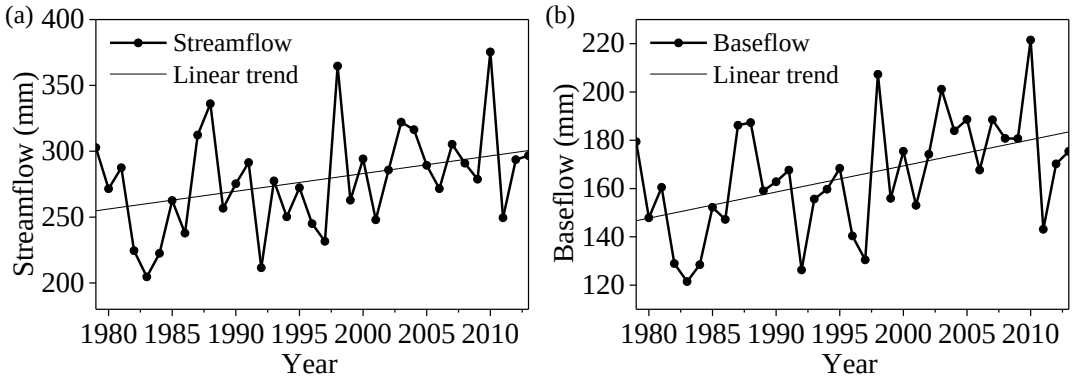

676

677 **Figure 4.** Variations of annual (a) streamflow and (b) baseflow from 1979 to 2013.

678

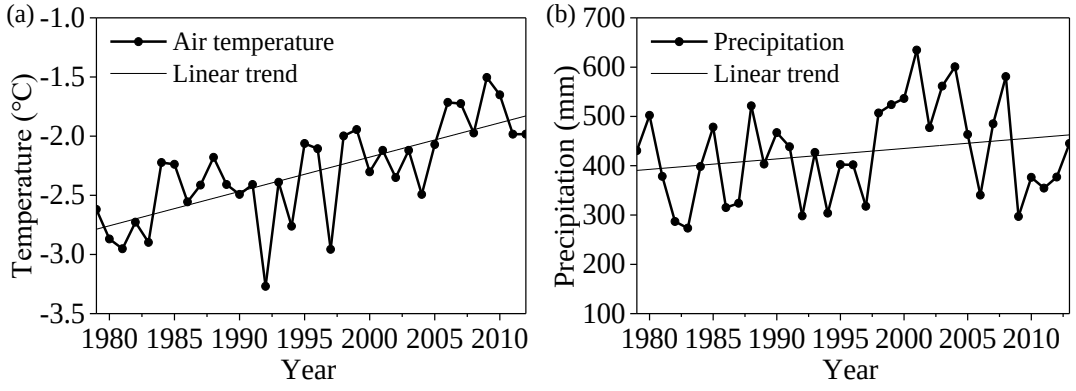

679

680 **Figure 5.** Variations of annual (a) mean air temperature and (b) precipitation from

681 1979 to 2013.

682

683

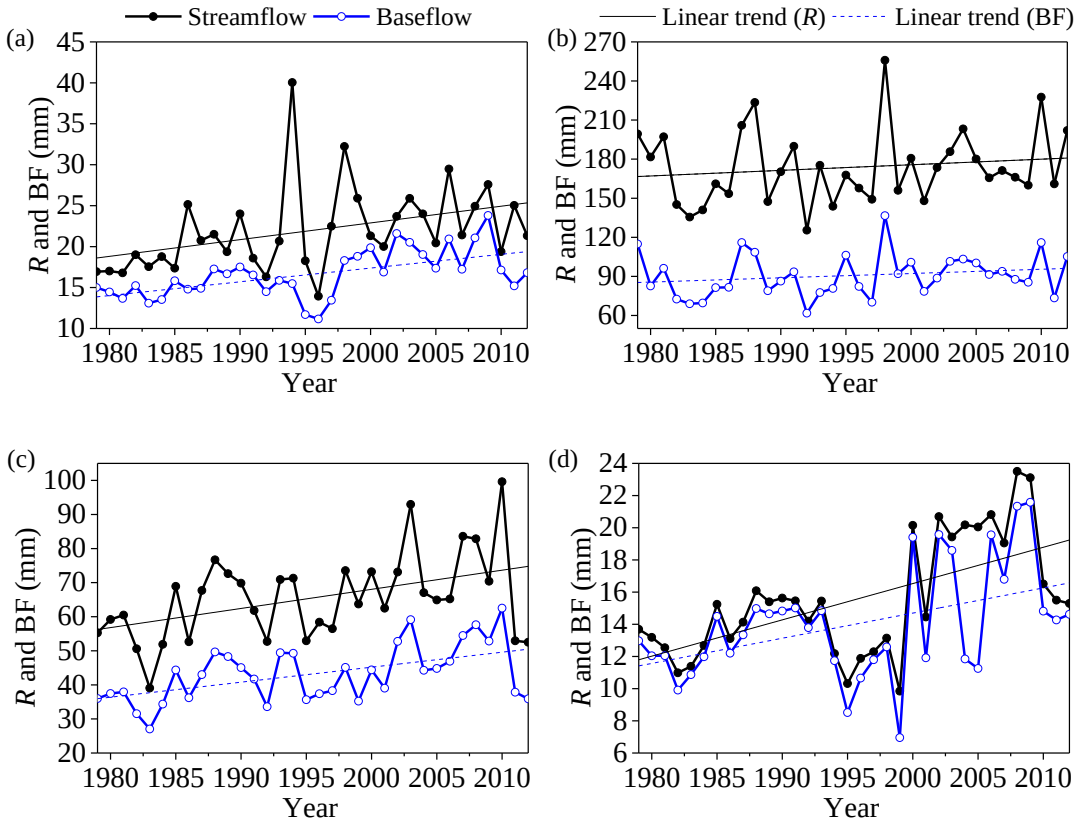

684

685 **Figure 6.** Variations of seasonal streamflow and baseflow in (a) spring, (b) summer,

686 (c) autumn, and (d) winter from 1979 to 2013.

687

688

689

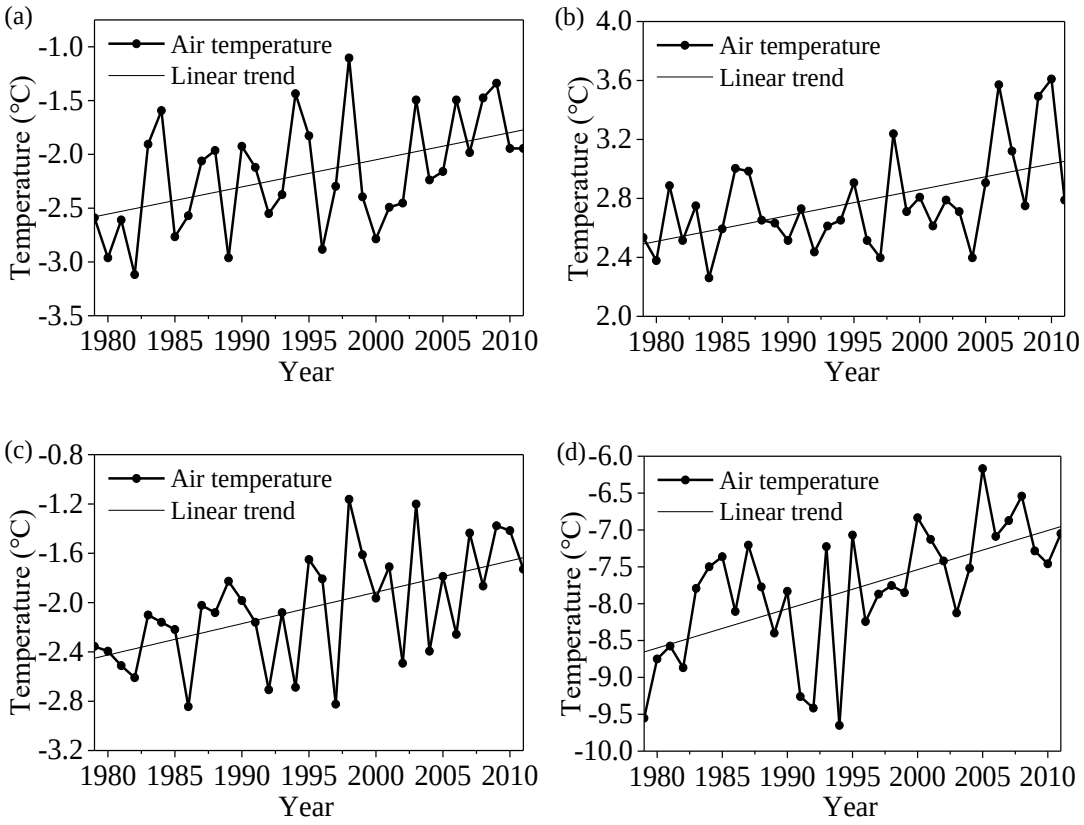

690

691 **Figure 7.** Variations of seasonal mean air temperature in (a) spring, (b) summer, (c)

692 autumn, and (d) winter from 1979 to 2013.

693

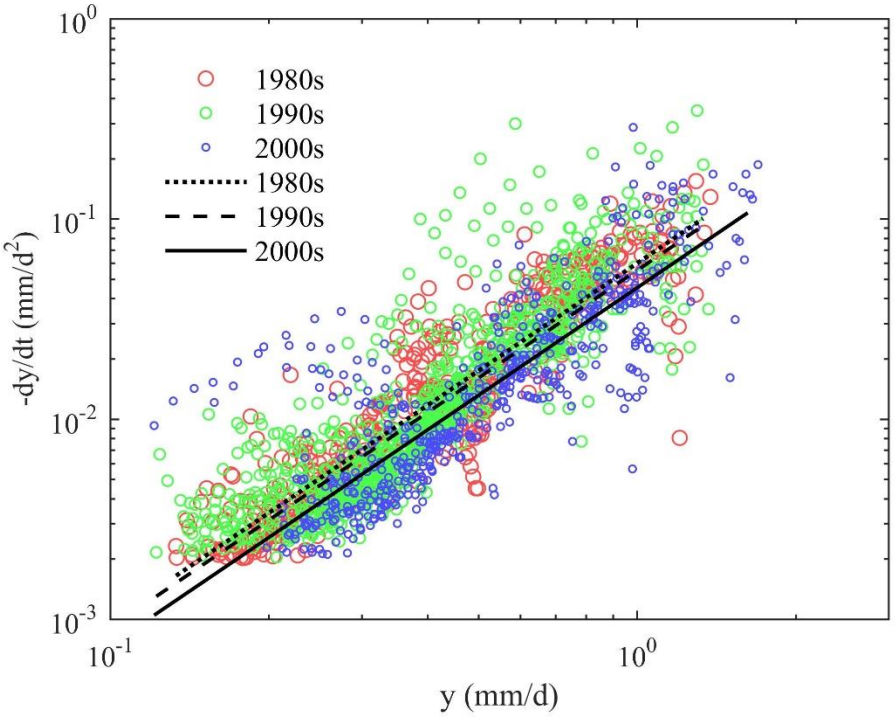

Figure 8. Recession data points of *-dy/dt* versus *y* and fitted recession curves by decades in log-log space. The black point line, dotted line, and solid line represent recession curves in the 1980s, 1990s, and 2000s, respectively.

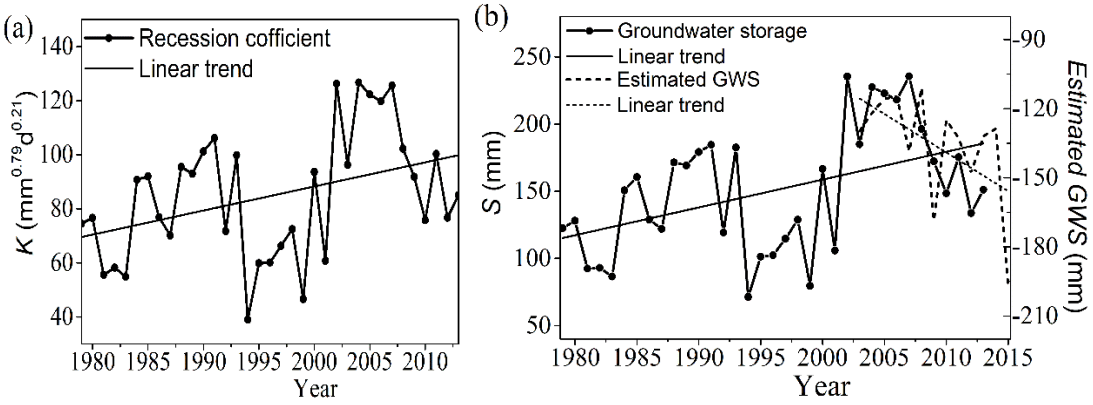

Figure 9. Variations of (a) the recession coefficient *K* and (b) the estimated groundwater storage *S* from 1979 to 2013 and the estimated groundwater storage change from 2003 to 2015 by GRACE data.

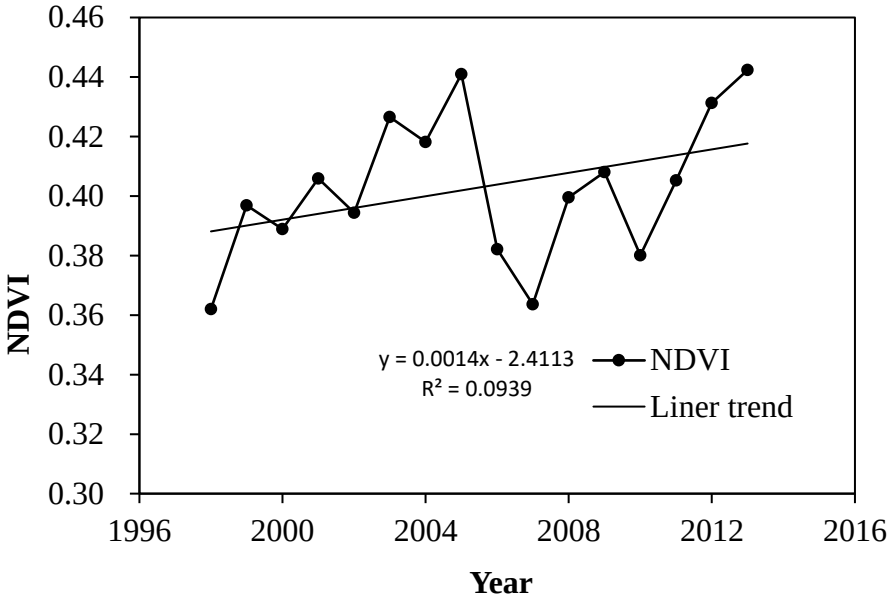

704

705 **Figure 10.** Variations of annual NDVI from 1998 to 2013 in the catchment.

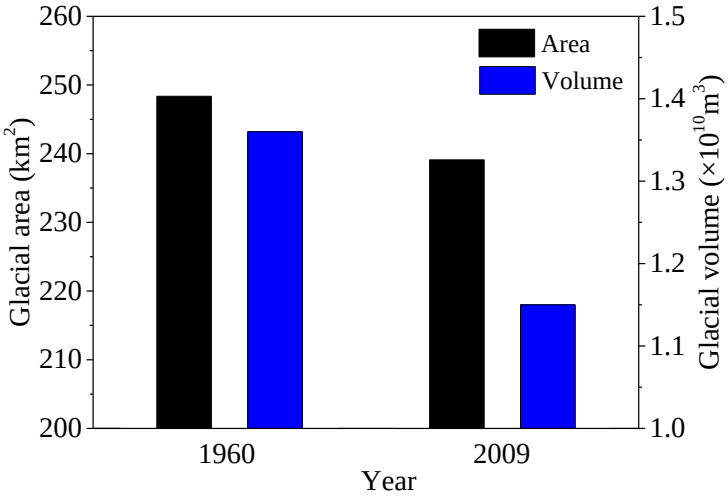

706

707 **Figure 11.** The total area and volume of glaciers in the Yangbajain Catchment in 1960

708 and 2009.

709